

Targeted Delivery of Gemcitabine for Precision Therapy of Cholangiocarcinoma Using Hyaluronic Acid-Modified Metal–Organic Framework Nanoparticles

Chuan Long,[△] Han Peng,[△] Wei Yang,[△] Min Wang, Bo Luo, Jie Hao, Yan Dong,^{*} and Wenwei Zuo^{*}



Cite This: *ACS Omega* 2024, 9, 11998–12005



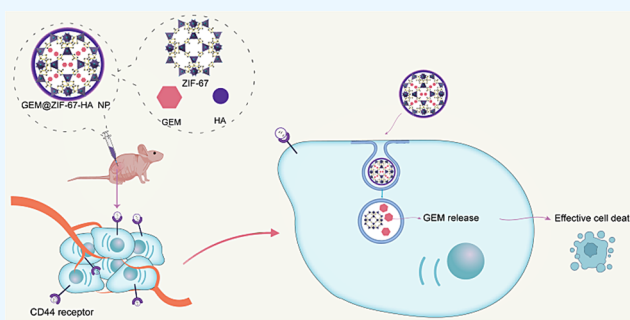
Read Online

ACCESS |

Metrics & More

Article Recommendations

ABSTRACT: Chemotherapy is widely recognized as an important approach for the treatment of cholangiocarcinoma. Gemcitabine (GEM) has been considered a first-line drug for treating cholangiocarcinoma due to its ability to effectively inhibit the proliferation, migration, and invasion of liver cancer cells. However, the systemic toxicity, premature degradation, and lack of tumor-targeting properties of GEM limit its application in cholangiocarcinoma chemotherapy. Additionally, precise targeted delivery of GEM is necessary to align with the current concept of precision medicine. In this study, considering the overexpression of hyaluronic acid (HA) receptors (CD44) on cholangiocarcinoma cells, we designed GEM@ZIF-67-HA NPs by loading GEM onto ZIF-67 and modifying its surface with HA. The structure, size, morphology, and elemental composition of GEM@ZIF-67-HA were analyzed using transmission electron microscopy, Fourier transform infrared spectroscopy, ζ -potential, and isothermal adsorption. Cell toxicity experiments demonstrated that GEM@ZIF-67-HA NPs not only reduced cytotoxicity to normal cells but also effectively inhibited the viability of two types of cholangiocarcinoma tumor cells. In a subcutaneous tumor model, GEM@ZIF-67-HA significantly suppressed tumor growth. The tumor-targeting and controllable properties of GEM@ZIF-67-HA NPs hold promise for further development in the strategy of precise targeted therapy for cholangiocarcinoma.



1. INTRODUCTION

Cholangiocarcinoma (CCA) is a common malignant tumor with a relatively low incidence rate in Europe and America but showing an increasing trend in China and Southeast Asia. However, the overall treatment level for CCA remains highly limited, and there is currently no ideal treatment method. Due to the late onset of clinical symptoms, early diagnosis is challenging. Moreover, CCA is anatomically located in a unique position and exhibits characteristics of infiltrating surrounding tissues, blood vessels, and nerves, resulting in a low feasibility of surgical resection, with only about 15–20% of cases eligible for surgical removal. The prognosis for cholangiocarcinoma is also very poor, with an average survival period of only 6 to 12 months.¹ In recent years, the incidence and mortality rates of CCA have been continuously increasing, highlighting the urgent need to develop more treatment methods to address this challenge.

Gemcitabine (GEM) is a deoxycytidine analogue that inhibits the synthesis of cellular DNA, thereby exhibiting antitumor effects. After entering the cell, gemcitabine can inhibit the elongation of DNA chains, leading to DNA breakage and cell apoptosis. It is widely used in the treatment of various malignant tumors.^{2,3} GEM alone or in combination

with cisplatin or doxorubicin has been reported as standard chemotherapy for advanced CCA patients.^{4,5} However, due to the significant resistance of CCA to traditional chemotherapy drugs, the prognosis for patients is poor. CCA exhibits drug resistance to treatment. Furthermore, increasing the dosage of chemotherapy drugs often fails to achieve satisfactory results and frequently leads to severe complications, including bone marrow suppression, neutropenia, leukopenia, and thrombocytopenia.^{6–8} This highlights the necessity of developing new treatment methods. To overcome the limitations of traditional treatment approaches, the development of nanoparticle (NP)-mediated drug delivery systems and novel drugs is needed.^{9–11}

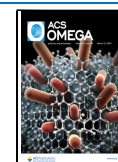
In the case of CCA patients, researchers are gradually focusing on more targeted and safer drugs, as well as comprehensive treatment methods such as biological and gene therapies.¹² Metal–organic frameworks (MOFs) have

Received: December 6, 2023

Revised: January 29, 2024

Accepted: February 9, 2024

Published: February 27, 2024



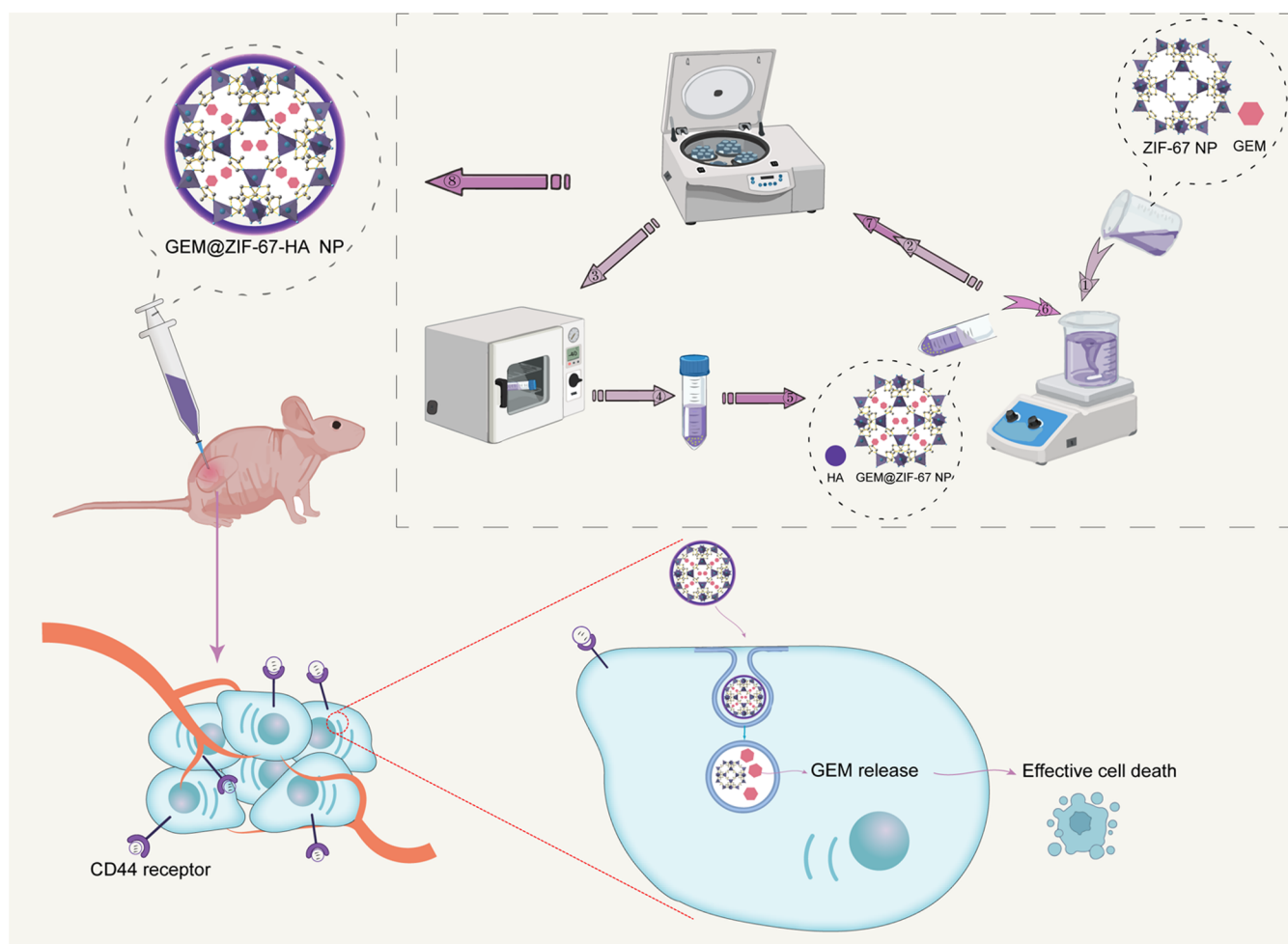


Figure 1. Schematic illustration of preparation of GEM@ZIF-67-HA NPs for treating cholangiocarcinoma.

been widely used in the field of drug delivery due to their ease of functionalization, tunable pore sizes, and flexible compositions. This is because MOFs can control particle size, surface chemistry, and internal porosity, enabling the design of complex materials based on MOFs. By adjusting the connectivity and pore size, MOFs with hydrophobic or hydrophilic properties can be designed to meet the specific physicochemical requirements of drugs or medical applications. However, there are currently some issues with drug delivery systems, including uncontrolled drug release, toxicity, and biocompatibility.^{13,14} Zeolitic imidazolate frameworks (ZIFs) are nanostructures with high adsorption capacity, controlled diffusion mechanisms, and thermal stability.¹⁵ Among them, ZIF-67, composed of a highly porous MOF with Co^{2+} and the organic linker 2-methylimidazole, has been extensively studied and considered an ideal candidate material in various fields. Compared to other nanocarriers, ZIF-67 offers higher pore volume and surface area, enhancing its ability as a drug carrier and resulting in more significant therapeutic effects.^{16,17}

Hyaluronic acid (HA) is a biodegradable, biocompatible, and nonimmunogenic glycosaminoglycan. As a major component of the extracellular matrix, HA has been extensively studied in biomedical and pharmaceutical applications. In particular, researchers have focused on utilizing HA as a targeting moiety in cancer therapy, as many types of tumor cells overexpress HA receptors, such as CD44.^{18,19} Due to its

multiple functional groups, HA can be chemically conjugated with anticancer drugs or nanocarriers for drugs/genes. HA-modified drug/nanocarrier systems have been developed to enhance the accumulation of drugs/cargos in cancer cells with high expression levels. In addition to its targeting functionality, HA-modified delivery systems can also enter cells more effectively through HA receptor-mediated endocytosis.^{20–22} Therefore, leveraging the CD44-HA-specific affinity has emerged as an attractive strategy for tumor-targeted therapy.

In this study, we proposed a method for the synthesis and characterization of GEM@ZIF-67-HA, where ZIF-67 NPs were functionalized with a combination of GEM chemotherapy drug and HA-specific ligand as a complex for targeted therapy to enhance the treatment efficacy for CCA (Figure 1). This strategy may represent a novel and effective treatment approach for CCA.

2. MATERIALS AND METHODS

2.1. Synthesis of ZIF-67. To synthesize ZIF-67,²³ $\text{Co}(\text{NO}_3)_2 \cdot 6\text{H}_2\text{O}$ (500 mg) was dissolved in 3 mL of distilled water, followed by the dissolution of 2-methylimidazole (6 g) in 25 mL of distilled water. The two solutions were mixed and vigorously stirred for 6 h at room temperature. The resulting mixture was then centrifuged at 10 000 rpm for 10 min to collect the purple precipitate. The precipitate was subsequently washed three times with distilled water and methanol. After drying at 80 °C for 24 h, the ZIF-67 NPs were ready for use.

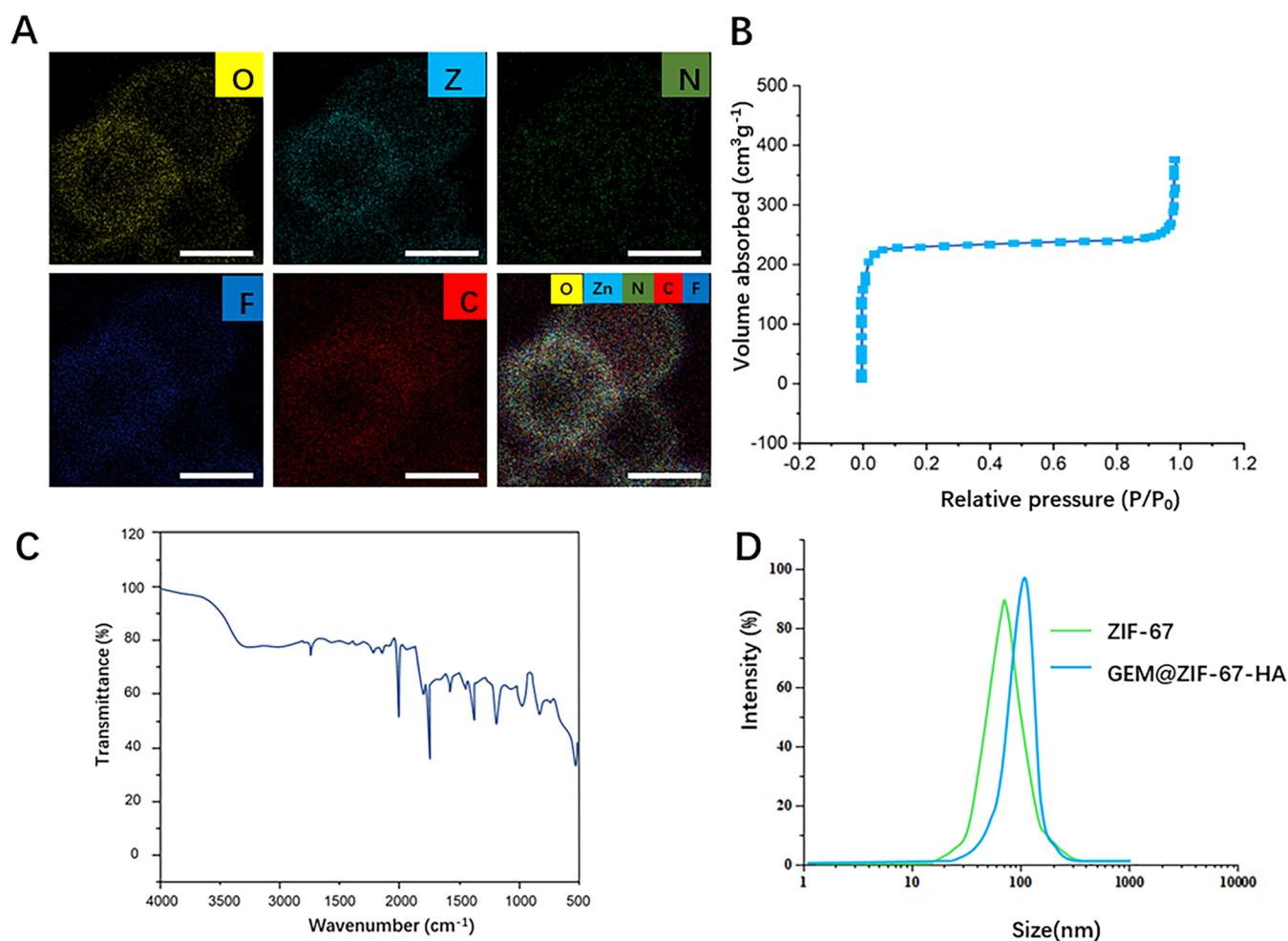


Figure 2. (A) Transmission electron micrograph and element mapping of GEM@ZIF-67-HA NPs. (B) Isothermal adsorption isotherm of GEM@ZIF-67-HA NPs. (C) FTIR spectrum of GEM@ZIF-67-HA NPs. (D) Particle size analysis of ZIF-67 NPs and GEM@ZIF-67-HA NPs. Scale bar = 100 nm.

2.2. Synthesis of GEM@ZIF-67-HA. First, about 50 mg of ZIF-67 powder was dehydrated under dynamic vacuum conditions overnight. Then, it was dissolved in 2 mL of GEM solution with a concentration of 2 mg per mL, which was prepared using deionized water. According to this ratio, theoretically, there is 2 mg of GEM in every 50 mL of ZIF-67. After stirring at room temperature for 1 h, the sample was centrifuged at 9000 rpm for 30 min. To remove any solvent, the sample was subjected to freeze-drying treatment. Next, 1.5 mg of HA was dissolved in 20 mL of deionized water containing 15 mg of GEM @ZIF-67-HA NPs. Then, the solution was stirred vigorously in the dark at room temperature for 24 h. Subsequently, the precipitate was separated by centrifugation and washed with deionized water at least 3 times to obtain the GEM @ZIF-67-HA NPs product.

2.3. Characterization. A range of characterization methods were utilized. Transmission electron microscopy (Talos F200C, Thermo Scientific) was employed to observe the morphology of GEM @ZIF-67-HA and confirm the successful loading of GEM into ZIF-67. Fourier transform infrared (FTIR) spectra were recorded using an FT/IR-4700 FTIR spectrometer (JASCO). Dynamic light scattering (DLS) (Malvern Zetasizer Nano-ZS90) was utilized to observe the particle size and ζ -potential of the GEM @ZIF-67-HA NPs.

2.4. Experimental Study on the Stability of GEM@ZIF-67-HA NPs. GEM@ZIF-67-HA NPs were diluted to a concentration of 0.1 mg/mL using PBS (pH = 7.4) buffer and 5% FBS-DMEM medium, respectively. The particle size was measured at 1, 2, 3, 4, 5, 6, and 7 days using a Malvern Zetasizer nanoparticle analyzer. Three readings were taken for each sample, and the average value was recorded as the result.

2.5. Release Studies of GEM from GEM@ZIF-67-HA. The 20 mg GEM@ZIF-67-HA NPs were uniformly dispersed in phosphate buffer solutions with different pH values (pH = 7.4, 6.5, 5.5). Then, the samples were centrifuged at specific time points (0, 2, 4, 6, 12, 18, 24 h), and the supernatant was collected for UV-vis analysis, and the cumulative release rate of GEM was calculated by equation.

2.6. Western Blotting Assay. Western blot is used to detect the expression of CD44 protein in cells. Cells are collected and lysed on ice for 30 min using RIPA buffer containing a protease inhibitor. The total protein is quantified according to the instructions of the BCA protein concentration determination kit. Protein samples are separated by gel electrophoresis and transferred onto a PVDF membrane. The membrane is then blocked in 5% BSA for 1 h and incubated overnight at 4 °C with the primary antibody against CD44 (1:1000). Subsequently, the membrane is incubated with the secondary antibody (1:5000) at room temperature for

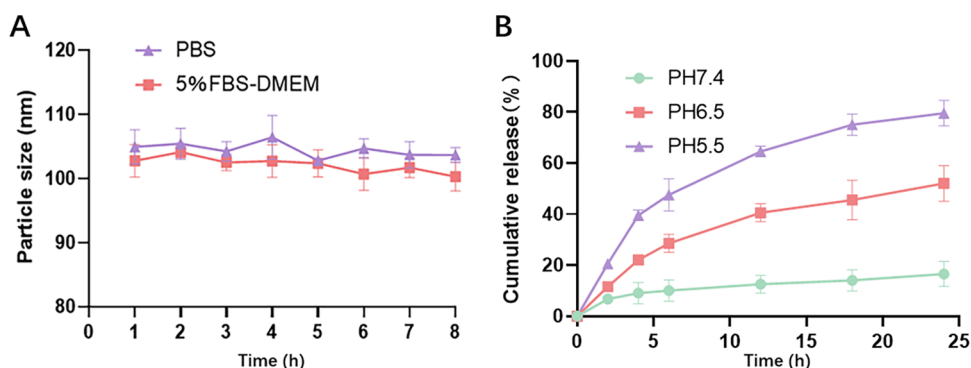


Figure 3. (A) Size variation of GEM@ZIF-67-HA NPs in PBS and 5% FBS-DMEM. (B) Cumulative GEM release from GEM@ZIF-67-HA NPs.

2 h, and the intensity of the bands is detected using a chemiluminescent substrate.

2.7. Cellular Uptake. QBC939 cells and HIBEC cells were seeded in a 6-well culture plate (5×10^5 cells/well). After incubation for 24 h, the cells were washed twice with PBS and then treated with $20 \mu\text{g}/2 \text{ mL}$ of Cy3-labeled GEM@ZIF-67-HA for 4 h. After that, the cells were washed twice with PBS to remove residual NPs and dead cells. The cells were then treated with 4% paraformaldehyde fixative solution for 30 min and stained with DAPI for 10 min to visualize the cell nuclei. Finally, the cells were observed under a confocal microscope.

2.8. Cytotoxicity Assay. The cell viability of HIBEC cells and QBC939 cells incubated with different concentrations of ZIF-67, GEM, GEM@ZIF-67, and GEM@ZIF-67-HA was measured using the cell counting kit-8 (CCK-8, Beyotime, China) according to the manufacturer's instructions. First, $100 \mu\text{L}$ of cell suspension (3×10^4 cells/mL) was seeded into 96-well plates and incubated with different concentrations of ZIF-67, GEM, GEM@ZIF-67, and GEM@ZIF-67-HA at 37°C for 48 h. Then, CCK-8 reagent ($10 \mu\text{L}$) was added to each well, and the mixture was further incubated at 37°C for an additional 1 h. The absorbance of the mixture at 450 nm was recorded, and the cell viability was calculated.

2.9. Establishment of Tumor Models. All experimental procedures and protocols were conducted in accordance with the guidelines of our institutional Animal Care and Use Committee, which were approved by the Department of Experimental Animal Science. Female BALB/c nude mice (6 weeks old, 18–20 g) were used for the experiments and housed in groups of 5 mice per cage under specific pathogen-free conditions ($22 \pm 2^\circ\text{C}$, $55 \pm 10\%$ humidity, 12 h–12 h light–dark cycle). A total of 1×10^7 QBC939 cells were inoculated on the right dorsal side of the mice. When the tumor volume reached approximately 80 mm^3 , $100 \mu\text{L}$ of free GEM group or GEM@ZIF-67-HA NPs was injected intravenously at a dose of 0.5 mg/kg. Tumor size was measured every 3 days, and no mice were excluded from the study.

Equation 1 was used to calculate the tumor volume.

$$\text{tumor volume} = (S^2 \times L)/2 \quad (1)$$

where “S” and “L”, respectively, represent the short axis and long axis of the tumor nodule.

2.10. Statistical Analysis. The statistical analysis was conducted using SPSS 24.0 software. The data were expressed as mean \pm standard deviation (SD). The Student's *t* test was used for comparisons between two groups, while one-way analysis of variance (ANOVA) was used for comparisons between three or more groups. A value of $P < 0.05$ was

considered statistically significant to indicate the presence of significant differences.

3. RESULTS AND DISCUSSION

3.1. Characterization and Performance Analysis of GEM@ZIF-67-HA NPs. After the synthesis of GEM@ZIF-67-HA NPs, we employed multiple techniques to assess their structure and properties. First, through the observation of TEM, we were able to determine the elemental composition and distribution of GEM@ZIF-67-HA NPs. Figure 2A displays representative TEM images of GEM@ZIF-67-HA NPs, which indicate good dispersion and morphology. Furthermore, we investigated the porous structure of GEM@ZIF-67-HA NPs using the isothermal adsorption method. Figure 2B illustrates the typical Type I isotherm of GEM@ZIF-67-HA NPs, indicating their mesoporous characteristics. This porous structure is crucial for drug loading and release, as it provides a larger surface area and improved drug diffusion properties. To evaluate the surface modification of GEM@ZIF-67-HA NPs, FTIR was employed, Figure 2C. In the spectrum, several characteristic peaks are observed. The peak at 138 cm^{-1} corresponds to the C–N stretching mode of 2-methylimidazole, the peak at 3326 cm^{-1} is associated with the N–H stretching vibration of GEM@ZIF-67, and the peak at 734 cm^{-1} is related to the C–H bending vibrations. These peaks indicate the surface modification of ZIF-67 and the loading of GEM. Moreover, the particle size of ZIF-67 NPs has significant implications for their biomedical applications. Smaller ZIF-67 NPs can more easily penetrate cell membranes, facilitating improved drug delivery. Through particle size analysis, we determined that the average particle size of prepared ZIF-67 NPs is approximately 69.7 nm. After loading GEM and surface modification with HA, the average volume of GEM@ZIF-67-HA increased to 103.6 nm^3 , with a dispersity index of 0.145 (Figure 2D). These findings provide foundational data for further research and application of GEM@ZIF-67-HA NPs in drug delivery.

3.2. pH-Responsive Release of GEM from GEM@ZIF-67-HA NPs. The stability experiment of GEM@ZIF-67-HA NPs showed that there was no significant change in the particle size over time in PBS or 5% FBS-DMEM medium, indicating the prepared nanoparticles possess good stability (Figure 3A). ZIFs are a subclass of metal–organic framework MOF materials composed of transition-metal ions and nitrogen-containing heterocyclic imidazole or purine organic ligands. ZIFs exhibit high porosity, relatively low cytotoxicity, and instability under acidic conditions.²⁴ Zhang et al. utilized pH-sensitive material ZIF-67 as a carrier to construct a pH-

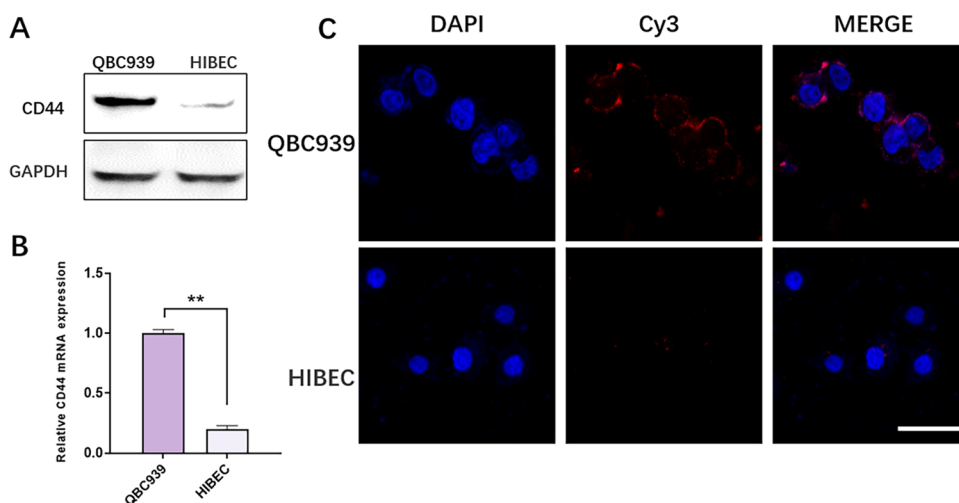


Figure 4. (A) Protein expression levels of CD44 in QBC939 cells and HIBEC cells. (B) mRNA expression levels of CD44 in QBC939 cells and HIBEC cells. (C) Cellular uptake study of Cy3-labeled GEM@ZIF-67-HA NPs in QBC939 cells and HIBEC cells. Scale bar: 50 μm.

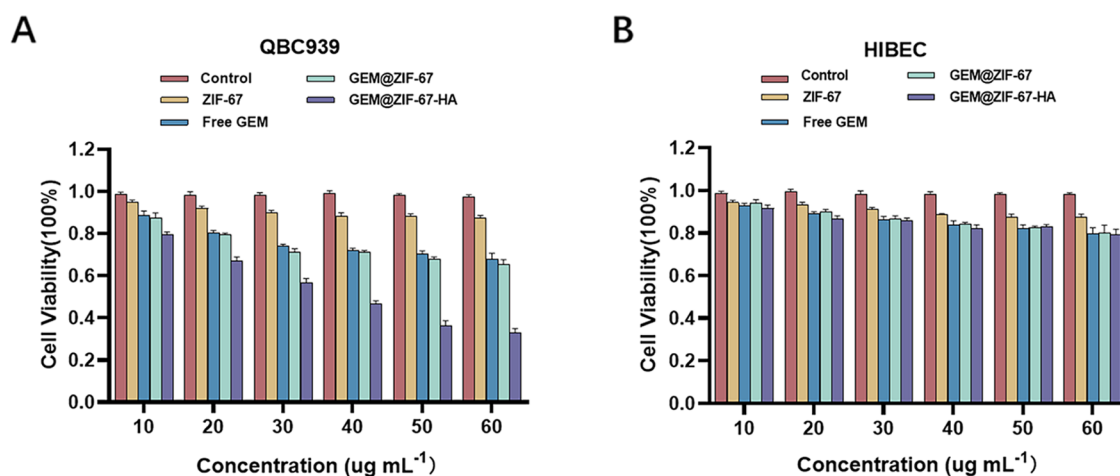


Figure 5. Viability of (A) QBC939 cells and (B) HIBEC cells determined by CCK-8 assay after incubation with ZIF-67, free GEM, GEM@ZIF-67, and GEM@ZIF-67-HA.

responsive nitrile imine nanodelivery system for intelligent and precise control of citrus gray mold disease.²⁵ Therefore, it is worthwhile to investigate the specific release behavior of GEM by constructing a pH-responsive delivery system based on ZIF-67. Due to its pH-sensitive dissolution properties, ZIF-67 has been applied in pH-controlled drug release systems.^{26,27} This study aimed to determine whether GEM@ZIF-67-HA NPs exhibit pH-responsive release of GEM. The pH in tumor tissue (5.5–6.0) is usually lower than the pH in normal tissue (7.4). As shown in Figure 3B, compared to the total GEM release of approximately 16.1% at pH 7.4, GEM@ZIF-67-HA NPs released up to 57.3% of GEM at pH 6.0, and 78.1% of GEM at pH 5.0. Thus, the anticancer drug GEM loaded in GEM@ZIF-67-HA NPs can exhibit pH-responsive release, specifically in the tumor tissue region of CCA.

3.3. In Vitro Tumor Cells Internalization. CD44, a transmembrane glycoprotein, is highly expressed in CCA cells. Studies have demonstrated that CD44 plays a critical role in the occurrence and progression of CCA.^{28–30} It regulates various biological behaviors of tumor cells, including proliferation, migration, and invasion, and is involved in the formation and modulation of the tumor microenvironment. Hence, CD44 has emerged as a potential target for the

diagnosis and treatment of CCA, and it can be utilized in research related to targeted therapy and immunotherapy.³¹ First, we measured the protein and mRNA expression levels of endogenous CD44 in CCA cell line QBC939 and the normal biliary epithelial cell line HIBEC (Figure 4A,4B). As expected, we observed significantly higher expression levels of CD44 in QBC939 cells compared to HIBEC cells, indicating the potential of CD44 as a targeting molecule. To evaluate the feasibility of targeted delivery using GEM@ZIF-67-HA NPs, we performed a cellular uptake study using Cy3-labeled GEM@ZIF-67-HA in QBC939 and HIBEC cells. As shown in Figure 4C, after coincubation of GEM@ZIF-67-HA with QBC939 cells for 4 h, we observed red fluorescence inside the cells, with significantly higher fluorescence intensity compared to HIBEC cells. This indicates the highly specific CD44 receptor binding capability of GEM@ZIF-67-HA NPs and their internalization through receptor-mediated endocytosis. Therefore, GEM@ZIF-67-HA NPs can accurately transport drugs into QBC939 cells and effectively enhance drug accumulation within the cells.

3.4. Cytotoxicity Assay. After verification, we found that GEM@ZIF-67-HA exhibits targeted effects on CCA cells. To evaluate the cytotoxicity of ZIF-67, GEM, GEM@ZIF-67, and

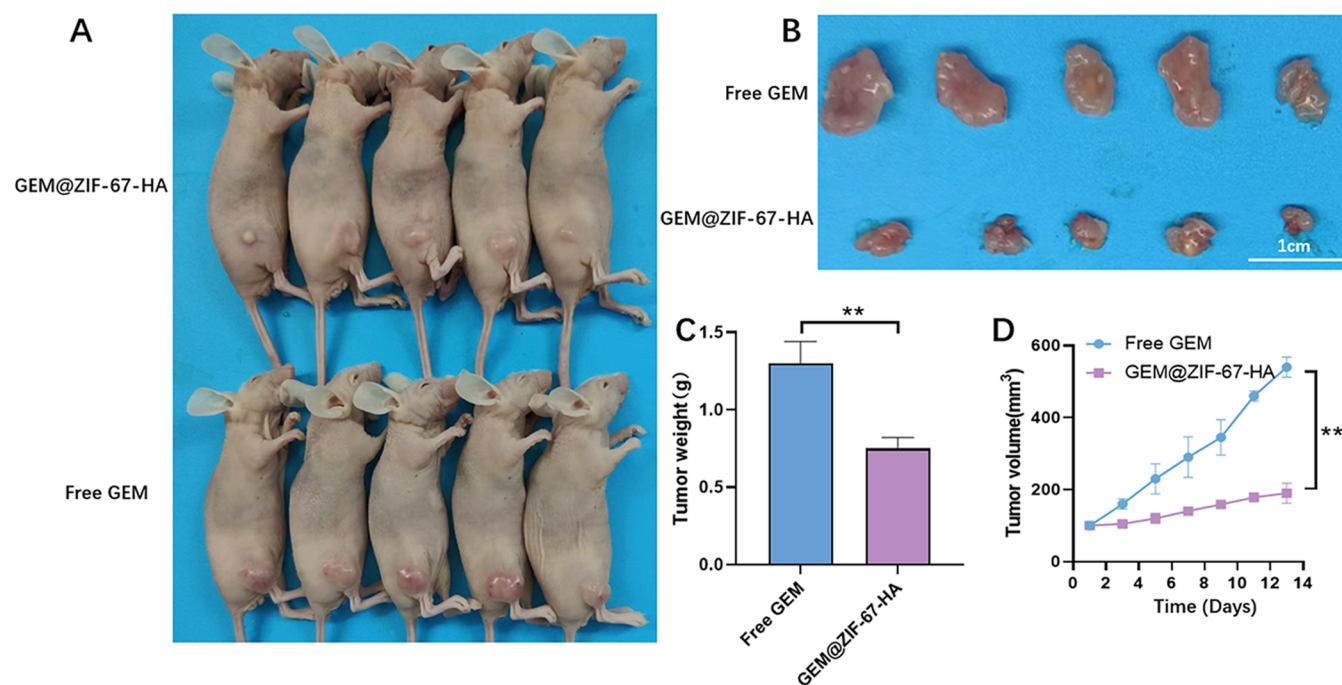


Figure 6. QBC939 tumor-bearing BALB/c nude mice were injected intravenously with C/Q@ZIF-8-HA. The tumor-bearing BALB/c nude mice were randomly divided into two groups: the free GEM group and the GEM@ZIF-67-HA group. (A, B) Tumors were collected from different groups after 14 days of treatment. The images of the tumors are displayed. (C) Tumor weights of different groups in QBC939 tumor-bearing BALB/c nude mice. (D) Tumor volumes of different groups in QBC939 tumor-bearing BALB/c nude mice. ** $P < 0.01$. Scale bar: 1 cm.

GEM@ZIF-67-HA at different concentrations on QBC939 and HIBEC cells, we conducted CCK-8 assays (Figure 5A,5B). Compared to the control group, we observed minimal effects of ZIF-67 on both QBC939 and HIBEC cells at a concentration of 50 $\mu\text{g/mL}$, with reductions of 3.12 and 4.98%, respectively. In comparison to the free GEM group, our research results showed a slight increase in cytotoxicity of GEM@ZIF-67 on QBC939 cells by 1.78% ($P = 0.44$), while a slight decrease in cytotoxicity was observed on HIBEC cells ($P = 0.65$). Furthermore, our cytotoxicity experiments revealed differences between GEM@ZIF-67 and GEM@ZIF-67-HA. The results showed that GEM@ZIF-67-HA significantly enhanced cytotoxicity on CCA cells at a concentration of 50 $\mu\text{g/mL}$, with a 21.3% higher cytotoxicity on QBC939 cells compared to the GEM@ZIF-67 group, while no significant difference was observed on HIBEC cells, with over 80% of HIBEC cells remaining viable. The above results indicate that GEM@ZIF-67-HA NPs have a significant inhibitory effect on tumor cells and low toxicity to normal cells. It has broad prospects for application in the treatment of CCA.

3.5. In Vivo Anticancer Assay. Inspired by the effectiveness of GEM@ZIF-67-HA in our in vitro studies, we further investigated the therapeutic potential of GEM@ZIF-67-HA for CCA in vivo through intravenous administration. To validate the efficacy of GEM@ZIF-67-HA in vivo for CCA, QBC939 cells were transplanted into BALB/c nude mice. The relative changes in tumor size and weight indicate the efficacy of different treatment strategies. The tumor formation rate in the free-GEM group was significantly faster than that in the GEM@ZIF-67-HA group (Figure 6A,B). After 14 days of injection, the tumor size and volume in the free-GEM group were significantly increased compared to the GEM@ZIF-67-HA group (Figure 6C,D). Overall, these results indicate that

GEM@ZIF-67-HA significantly inhibits the proliferative capacity of cholangiocarcinoma cells in tumor-bearing mice.

4. CONCLUSIONS

In summary, we successfully prepared GEM@ZIF-67-HA NPs and applied them in the treatment strategy for CCA. The presence of HA in the system resulted in good tumor cell targeting. Due to the high storage capacity and pH responsiveness of ZIF-67, the drug loading efficiency of GEM was 16.5 wt %, and GEM@ZIF-67-HA released 78.1% of GEM at pH 5.5. In in vivo experiments, compared to the free-GEM group, GEM@ZIF-67-HA significantly suppressed the growth of CCA in mice. These results suggest that the prepared GEM@ZIF-67-HA NPs, which possess targeted delivery and pH-responsive release of GEM, are a promising approach for the treatment of CCA. We anticipate that further clinical efficacy evaluation and appropriate structural modifications of GEM@ZIF-67-HA will provide more valuable insights into the therapeutic potential of GEM for CCA.

■ ASSOCIATED CONTENT

Data Availability Statement

All data generated or analyzed during this study are included in this published article.

■ AUTHOR INFORMATION

Corresponding Authors

Wenwei Zuo – Department of General Surgery, Affiliated Hospital of Chengdu University of Traditional Chinese Medicine, Chengdu 610000, China; Email: 942192101@qq.com

Yan Dong – Department of Oncology, Southwest Hospital, Army Medical University, Chongqing 400038, China; Email: yandong@tmmu.edu.cn

Authors

Chuan Long – Department of Otolaryngology, Affiliated Hospital of Chengdu University of Traditional Chinese Medicine, Chengdu 610000, China

Han Peng – Department of Oncology, Southwest Hospital, Army Medical University, Chongqing 400038, China;
orcid.org/0009-0009-4666-6936

Wei Yang – Department of Radiology, Affiliated Hospital of Chengdu University of Traditional Chinese Medicine, Chengdu 610000, China

Min Wang – Department of General Surgery, Affiliated Hospital of Chengdu University of Traditional Chinese Medicine, Chengdu 610000, China

Bo Luo – Department of General Surgery, Affiliated Hospital of Chengdu University of Traditional Chinese Medicine, Chengdu 610000, China

Jie Hao – Department of Oncology, Southwest Hospital, Army Medical University, Chongqing 400038, China

Complete contact information is available at:

<https://pubs.acs.org/10.1021/acsomega.3c09751>

Author Contributions

[△]C.L., H.P., and W.Y. contributed equally.

Notes

The authors declare no competing financial interest. Animal experiments were in accordance with the regulations of the Animal Ethical and Welfare Committee of Army Medical University.

ACKNOWLEDGMENTS

This work was supported by The General Program of Chongqing Natural Science Foundation, China (CSTB2023NSCQ-MSX0596).

REFERENCES

- (1) Morement, H.; Khuntikeo, N. Community Awareness and Education: In the West and Southeast Asia. In *Liver Fluke, Opisthorchis viverrini Related Cholangiocarcinoma: Liver Fluke Related Cholangiocarcinoma*; Springer International Publishing: Cham, 2023; Vol. 219, pp 349–359.
- (2) Shetty, A.; Nagesh, P. K. B.; Setua, S.; Hafeez, B. B.; Jaggi, M.; Yallapu, M. M.; Chauhan, S. C. Novel Paclitaxel Nanoformulation Impairs De Novo Lipid Synthesis in Pancreatic Cancer Cells and Enhances Gemcitabine Efficacy. *ACS Omega* **2020**, *5* (15), 8982–8991.
- (3) Zhou, S.; Shang, Q.; Wang, N.; Li, Q.; Song, A.; Luan, Y. Rational design of a minimalist nanoplatform to maximize immunotherapeutic efficacy: Four birds with one stone. *J. Controlled Release* **2020**, *328*, 617–630, DOI: 10.1016/j.jconrel.2020.09.035.
- (4) Moris, D.; Palta, M.; Kim, C.; Allen, P. J.; Morse, M. A.; Lidsky, M. E. Advances in the treatment of intrahepatic cholangiocarcinoma: An overview of the current and future therapeutic landscape for clinicians. *Ca-Cancer J. Clin.* **2023**, *73* (2), 198–222, DOI: 10.3322/caac.21759.
- (5) Han, H.; Li, S.; Zhong, Y.; Huang, Y.; Wang, K.; Jin, Q.; Ji, J.; Yao, K. Emerging pro-drug and nano-drug strategies for gemcitabine-based cancer therapy. *Asian J. Pharm. Sci.* **2022**, *17* (1), 35–52, DOI: 10.1016/j.ajps.2021.06.001.
- (6) Paroha, S.; Verma, J.; Dubey, R. D.; Dewangan, R. P.; Molugulu, N.; Bapat, R. A.; Sahoo, P. K.; Kesharwani, P. Recent advances and prospects in gemcitabine drug delivery systems. *Int. J. Pharm.* **2021**, *592*, No. 120043.
- (7) Kobayashi, S.; Terashima, T.; Shiba, S.; Yoshida, Y.; Yamada, I.; Iwadou, S.; Horiguchi, S.; Takahashi, H.; Suzuki, E.; Moriguchi, M.; Tsuji, K.; Otsuka, T.; Asagi, A.; Kojima, Y.; Takada, R.; Morizane, C.; Mizuno, N.; Ikeda, M.; Ueno, M.; Furuse, J. Multicenter retrospective analysis of systemic chemotherapy for unresectable combined hepatocellular and cholangiocarcinoma. *Cancer Sci.* **2018**, *109* (8), 2549–2557.
- (8) Cheon, J.; Lee, C. K.; Sang, Y. B.; Choi, H. J.; Kim, M. H.; Ji, J. H.; Ko, K. H.; Kwon, C. I.; Kim, D. J.; Choi, S. H.; Kim, C.; Kang, B.; Chon, H. J. Real-world efficacy and safety of nab-paclitaxel plus gemcitabine-cisplatin in patients with advanced biliary tract cancers: a multicenter retrospective analysis. *Ther. Adv. Med. Oncol.* **2021**, *13*, No. 17588359211035983.
- (9) Oh, D. Y.; Lee, K. H.; Lee, D. W.; Yoon, J.; Kim, T. Y.; Bang, J. H.; Nam, A. R.; Oh, K. S.; Kim, J. M.; Lee, Y.; Guthrie, V.; McCoon, P.; Li, W.; Wu, S.; Zhang, Q.; Rebelatto, M. C.; Kim, J. W. Gemcitabine and cisplatin plus durvalumab with or without tremelimumab in chemotherapy-naïve patients with advanced biliary tract cancer: an open-label, single-centre, phase 2 study. *Lancet Gastroenterol. Hepatol.* **2022**, *7* (6), 522–532, DOI: 10.1016/S2468-1253(22)00043-7.
- (10) Martin, J. D.; Cabral, H.; Stylianopoulos, T.; Jain, R. K. Improving cancer immunotherapy using nanomedicines: progress, opportunities and challenges. *Nat. Rev. Clin. Oncol.* **2020**, *17* (4), 251–266.
- (11) Spadea, A.; Rios de la Rosa, J. M.; Tirella, A.; Ashford, M. B.; Williams, K. J.; Stratford, I. J.; Tirelli, N.; Mehibel, M. Evaluating the Efficiency of Hyaluronic Acid for Tumor Targeting via CD44. *Mol. Pharmaceutics* **2019**, *16* (6), 2481–2493.
- (12) Michalczyk, M.; Humeniuk, E.; Adamczuk, G.; Korga-Plewko, A. Hyaluronic Acid as a Modern Approach in Anticancer Therapy-Review. *Int. J. Mol. Sci.* **2023**, *24* (1), 103 DOI: 10.3390/ijms24010103.
- (13) Joseph, N. M.; Tsokos, C. G.; Umetsu, S. E.; Shain, A. H.; Kelley, R. K.; Onodera, C.; Bowman, S.; Talevich, E.; Ferrell, L. D.; Kakar, S.; Krings, G. Genomic profiling of combined hepatocellular-cholangiocarcinoma reveals similar genetics to hepatocellular carcinoma. *J. Pathol.* **2019**, *248* (2), 164–178.
- (14) Luo, Z.; Sheng, Y.; Jiang, C.; Pan, Y.; Wang, X.; Nezamzadeh-Ejehieh, A.; Ouyang, J.; Lu, C.; Liu, J. Recent advances and prospects of metal-organic frameworks in cancer therapies. *Dalton Trans.* **2023**, *52* (47), 17601–17622, DOI: 10.1039/D3DT02543H.
- (15) Zhang, D.; Liu, D.; Wang, C.; Su, Y.; Zhang, X. Nanoreactor-based catalytic systems for therapeutic applications: Principles, strategies, and challenges. *Adv. Colloid Interface Sci.* **2023**, *322*, No. 103037.
- (16) Huang, J.; Xu, Z.; Jiang, Y.; Law, W. C.; Dong, B.; Zeng, X.; Ma, M.; Xu, G.; Zou, J.; Yang, C. Metal organic framework-coated gold nanorod as an on-demand drug delivery platform for chemophothermal cancer therapy. *J. Nanobiotechnol.* **2021**, *19* (1), 219.
- (17) Zeng, Y.; Liao, D.; Kong, X.; Huang, Q.; Zhong, M.; Liu, J.; Nezamzadeh-Ejehieh, A.; Pan, Y.; Song, H. Current status and prospect of ZIF-based materials for breast cancer treatment. *Colloids Surf., B* **2023**, *232*, No. 113612, DOI: 10.1016/j.colsurfb.2023.113612.
- (18) Zheng, H.; Zhang, Y.; Liu, L.; Wan, W.; Guo, P.; Nyström, A. M.; Zou, X. One-pot Synthesis of Metal-Organic Frameworks with Encapsulated Target Molecules and Their Applications for Controlled Drug Delivery. *J. Am. Chem. Soc.* **2016**, *138* (3), 962–968.
- (19) Chiesa, E.; Greco, A.; Riva, F.; Dorati, R.; Conti, B.; Modena, T.; Genta, I. CD44-Targeted Carriers: The Role of Molecular Weight of Hyaluronic Acid in the Uptake of Hyaluronic Acid-Based Nanoparticles. *Pharmaceutics* **2022**, *15* (1), No. 103, DOI: 10.3390/ph15010103.
- (20) Chiesa, E.; Dorati, R.; Conti, B.; Modena, T.; Cova, E.; Meloni, F.; Genta, I. Hyaluronic Acid-Decorated Chitosan Nanoparticles for CD44-Targeted Delivery of Everolimus. *Int. J. Mol. Sci.* **2018**, *19* (8), No. 2310, DOI: 10.3390/ijms19082310.
- (21) Liang, Y.; Wang, Y.; Wang, L.; Liang, Z.; Li, D.; Xu, X.; Chen, Y.; Yang, X.; Zhang, H.; Niu, H. Self-crosslinkable chitosan-hyaluronic acid dialdehyde nanoparticles for CD44-targeted siRNA delivery to treat bladder cancer. *Bioact. Mater.* **2021**, *6* (2), 433–446.

(22) Rios de la Rosa, J. M.; Pingraja, P.; Pelliccia, M.; Spadea, A.; Lallana, E.; Gennari, A.; Stratford, I. J.; Rocchia, W.; Tirella, A.; Tirelli, N. Binding and Internalization in Receptor-Targeted Carriers: The Complex Role of CD44 in the Uptake of Hyaluronic Acid-Based Nanoparticles (siRNA Delivery). *Adv. Healthcare Mater.* **2019**, *8* (24), No. e1901182.

(23) Pan, D. C.; Krishnan, V.; Salinas, A. K.; Kim, J.; Sun, T.; Ravid, S.; Peng, K.; Wu, D.; Nurunnabi, M.; Nelson, J. A.; Niziolek, Z.; Guo, J.; Mitragotri, S. Hyaluronic acid-doxorubicin nanoparticles for targeted treatment of colorectal cancer. *Bioeng. Transl. Med.* **2021**, *6* (1), No. e10166.

(24) Zheng, Z.; Rong, Z.; Nguyen, H. L.; Yaghi, O. M. Structural Chemistry of Zeolitic Imidazolate Frameworks. *Inorg. Chem.* **2023**, *62* (51), 20861–20873.

(25) Zhang, X.; Tang, X.; Zhao, C.; Yuan, Z.; Zhang, D.; Zhao, H.; Yang, N.; Guo, K.; He, Y.; He, Y.; Hu, J.; He, L.; He, L.; Qian, K. A pH-responsive MOF for site-specific delivery of fungicide to control citrus disease of *Botrytis cinerea*. *Chem. Eng. J.* **2022**, *431*, No. 133351.

(26) Wu, J.; Zhang, Z.; Qiao, C.; Yi, C.; Xu, Z.; Chen, T.; Dai, X. Synthesis of Monodisperse ZIF-67@CuSe@PVP Nanoparticles for pH-Responsive Drug Release and Photothermal Therapy. *ACS Biomater. Sci. Eng.* **2022**, *8* (1), 284–292.

(27) de Moura Ferraz, L. R.; Tabosa, A.É. G. A.; da Silva Nascimento, D. D. S.; Ferreira, A. S.; Silva, J. Y. R.; Junior, S. A.; Rolim, L. A.; Rolim-Neto, P. J. Benzimidazole in vitro dissolution release from a pH-sensitive drug delivery system using Zif-8 as a carrier. *J. Mater. Sci.: Mater. Med.* **2021**, *32* (6), 59.

(28) Hassn Mesrati, M.; Syafruddin, S. E.; Mohtar, M. A.; Syahir, A. CD44: A Multifunctional Mediator of Cancer Progression. *Biomolecules* **2021**, *11* (12), 1850 DOI: [10.3390/biom11121850](https://doi.org/10.3390/biom11121850).

(29) Suwannakul, N.; Ma, N.; Midorikawa, K.; Oikawa, S.; Kobayashi, H.; He, F.; Kawanishi, S.; Murata, M. CD44v9 Induces Stem Cell-Like Phenotypes in Human Cholangiocarcinoma. *Front. Cell Dev. Biol.* **2020**, *8*, 417 DOI: [10.3389/fcell.2020.00417](https://doi.org/10.3389/fcell.2020.00417).

(30) Bei, Y.; He, J.; Dong, X.; Wang, Y.; Wang, S.; Guo, W.; Cai, C.; Xu, Z.; Wei, J.; Liu, B.; Zhang, N.; Shen, P. Targeting CD44 Variant 5 with an Antibody-Drug Conjugate Is an Effective Therapeutic Strategy for Intrahepatic Cholangiocarcinoma. *Cancer Res.* **2023**, *83* (14), 2405–2420.

(31) Cheng, M.; Liang, G.; Yin, Z.; Lin, X.; Sun, Q.; Liu, Y. Immunosuppressive role of SPP1-CD44 in the tumor microenvironment of intrahepatic cholangiocarcinoma assessed by single-cell RNA sequencing. *J. Cancer Res. Clin. Oncol.* **2023**, *149* (9), 5497–5512.